European Journal of Cardio-Thoracic Surgery 57 (2020) 588–595
doi:10.1093/ejcts/ezz246 Advance Access publication 18 September 2019

ORIGINAL ARTICLE

Cite this article as: Schäfer M, Barker AJ, Jaggers J, Morgan GJ, Stone ML, Truong U *et al.* Abnormal aortic flow conduction is associated with increased viscous energy loss in patients with repaired tetralogy of Fallot. Eur J Cardiothorac Surg 2020;57:588–95.

Abnormal aortic flow conduction is associated with increased viscous energy loss in patients with repaired tetralogy of Fallot

Michal Schäfer [a,*], Alex J. Barker [b,c], James Jaggers [c], Gareth J. Morgan [a], Matthew L. Stone[c], Uyen Truong[a], Lorna P. Browne[b], Ladonna Malone [b], D. Dunbar Ivy [a] and Max B. Mitchell [d]

[a] Division of Cardiology, Department of Pediatrics, Heart Institute, Children's Hospital Colorado, University of Colorado Denver, Anschutz Medical Campus, Aurora, CO, USA
[b] Department of Radiology, Children's Hospital Colorado, University of Colorado Denver, Anschutz Medical Campus, Aurora, CO, USA
[c] Department of Bioengineering, University of Colorado Denver, Anschutz Medical Campus, Aurora, CO, USA
[d] Department of Surgery, Section of Congenital Heart Surgery, Heart Institute, Children's Hospital Colorado, University of Colorado Denver, Anschutz Medical Campus, Aurora, CO, USA

* Corresponding author. Division of Cardiology, Department of Pediatrics, Heart Institute, Children's Hospital Colorado, University of Colorado Denver, Anschutz Medical Campus, 13123E 16th Ave, Aurora CO 80045-2560, USA. Tel: +1-720-7777290; e-mail: michal.schafer@ucdenver.edu (M. Schäfer).

Received 13 June 2019; received in revised form 29 July 2019; accepted 13 August 2019

Key question

What are the flow haemodynamic characteristics in the thoracic aorta in tetralogy of Fallot (TOF)?

Key finding(s)

TOF is associated with abnormal aortic flow associated with increased viscous energy loss.

Take-home message

TOF-related aortopathy is associated with abnormal flow conduction similar to that of bicuspid aortic valve aortopathies.

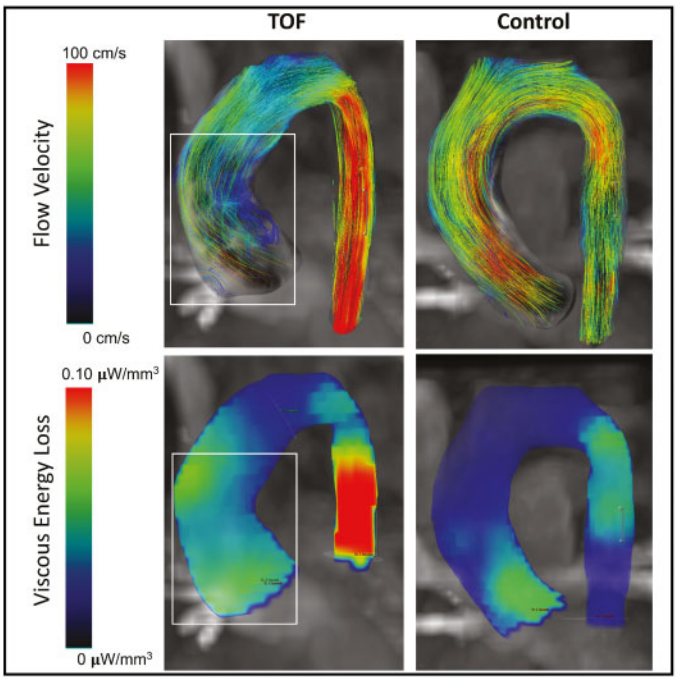

Abstract

OBJECTIVES: Aortopathy in tetralogy of Fallot (TOF) is characterized by increased aortic stiffness, dilation and reduced left ventricular (LV) function. Repair in infancy normalizes aortic dimensions in early childhood. Our prior work demonstrated that early TOF repair does not normalize aortic compliance and that abnormal ascending aortic flow patterns are prevalent. The objectives of this study were to: (i) determine whether proximal aortic flow-mediated viscous energy loss (E_L') is elevated in patients with early TOF repair compared with healthy controls, and (ii) determine whether the degree of E_L' is associated with LV function.

METHODS: Forty-one patients post TOF repair with normalized aortic size and 15 healthy controls underwent 4-dimenisonal-flow magnetic resonance imaging flow analysis and E_L' assessment. Correlations between E_L', aortic size, and LV function were assessed.

RESULTS: The TOF group had increased peak systolic thoracic aorta E'_L (3.8 vs 1.5 mW, $P = 0.004$) and increased averaged E'_L throughout the cardiac cycle (1.2 vs 0.5 mW, $P = 0.003$). Peak and mean systolic E'_L in the ascending aorta was increased 2-fold in the TOF group compared with control (peak: 2.0 vs 0.9 mW, $P = 0.007$). Peak E'_L measured along the entire thoracic aortic length correlated with LV ejection fraction (R = -0.45, $P = 0.009$), indexed LV end-systolic volume (R = -0.40, $P = 0.010$), and right ventricular end-systolic volume (R = -0.37, $P = 0.034$).

CONCLUSIONS: Patients with repaired TOF exhibit abnormal aortic flow associated with increased E'_L in the thoracic aorta. The magnitude of E'_L is associated with LV function and volumes. Increased aortic E'_L in TOF is likely due to inherently abnormal LV outflow geometry and or right ventricular interaction. Reduced aortic flow efficiency in TOF increases cardiac work and may be an important factor in long-term cardiac performance.

Keywords: Tetralogy of Fallot • Aorta • 4D-flow MRI

ABBREVIATIONS

LV	Left ventricular
LVEF	Left ventricular ejection fraction
LVOT	Left ventricular outflow tract
MRI	Magnetic resonance imaging
RV	Right ventricular
TOF	Tetralogy of Fallot

INTRODUCTION

Conotruncal anomalies present with structural features influence the natural history, initial surgical treatment and late management of these lesions. Aortopathy is an underappreciated comorbidity with ill-defined long-term consequences, particularly in the current era of early surgical repair. In tetralogy of Fallot (TOF), the most common conotruncal lesion, numerous studies have reported abnormal ascending aortic wall histopathology, physiology and haemodynamic perturbations [1–3]. The histopathology of TOF-associated aortopathy resembles Marfan's syndrome and is characterized by medial degeneration [2, 4]. Non-invasive and invasive studies have reported increased aortic stiffness in TOF patients that directly correlates with the degree of aortic dilation [5, 6]. Putative aetiologies of TOF-associated aortopathy include early chronic aortic volume overload, intrinsic genetic abnormalities and combinations of these factors [5–8].

Several groups have shown that complete TOF repair in infancy normalizes proximal aortic dimensions in early childhood [9]. In a recent report, we assessed comprehensive aortic flow haemodynamics with 4-dimensional (4D)-flow magnetic resonance imaging (MRI) in a group of preadolescent TOF patients who underwent complete repair prior to age 1 year [3]. Compared with age-matched normal controls, the TOF group had increased aortic wall shear stress and stiffness despite all TOF subjects having normal aortic dimensions. In addition, there was a high prevalence of pathological flow formations in the ascending aorta regardless of arch sidedness. Other investigators have correlated increased aortic wall stiffness with reduced left ventricular (LV) function in both children and adults with repaired TOF [5, 10]. Elevated wall stiffness in other aortopathies is associated with secondary flow patterns consisting of complex supraphysiological vortical and helical flow structures that increase energy dissipation and myocardial workload [11, 12]. However, comparative analysis of secondary flow haemodynamic structures using qualitative approaches is difficult due to differences in vessel geometry and the complexity of observed flow structures.

4D-flow MRI enables quantification of instantaneous viscous energy loss (E'_L) across a defined vascular pathway. E'_L therefore serves as a marker of prominent secondary aortic flow structures that manifest in the form of complex 3-dimensional helical or vortical structures [12, 13]. Based on our prior findings, we hypothesized that patients with TOF have abnormal flow conduction through the ascending aorta that is associated with the increased dissipated aortic E'_L. The objectives of this study were: (i) to quantify ascending aortic E'_L in patients who previously underwent complete TOF repair, (ii) to compare aortic E'_L in TOF patients to normal controls with similar age distribution and (iii) to determine if aortic E'_L is associated with aortic size and LV function.

METHODS

As part of a larger retrospective study, we identified 41 paediatric and adult patients with repaired TOF who underwent comprehensive clinically indicated cardiac MRI for the evaluation of right ventricular outflow tract pathology [3]. Patients with abnormal aortic valve anatomy or function, residual ventricular septal defect and dilated ascending aorta (z-score >2) were excluded to eliminate other lesions that impact aortic flow haemodynamics. Fifteen healthy volunteers of similar age and body surface area and having morphologically normal aortas were recruited from different studies considering the software/hardware optimization. This retrospective study was approved by the Colorado Multiple Institutional Review Board with waived written consent information.

Magnetic resonance imaging protocol

MRI evaluation was performed with a 1.5 T or 3.0 T system (Achieva/Ingenia, Philips Medical Systems, Best, Netherlands) using a 32-channel coil. Ventricular and functional analyses were performed using standard prescribed 2-dimensional cine bSSFP short-, long- and 4-chamber axis images acquired during end-expiratory breath holds. As a part of the standard evaluation, patients with repaired TOF received contrast enhanced angiography for the dimensional analysis of the right ventricle, right ventricular outflow tract and aorta.

E'_L and qualitative flow haemodynamic analysis were performed using 4D-flow MRI acquired in a sagittally oriented field of view covering the mid-thorax with retrospective gating and pencil beam respiratory navigation tracking the lung–liver interface. Typical scan parameters were: echo time 2.4–2.6 ms, repetition times = 4.2–5.0 ms, flip angle = 10°, 14 cardiac phases

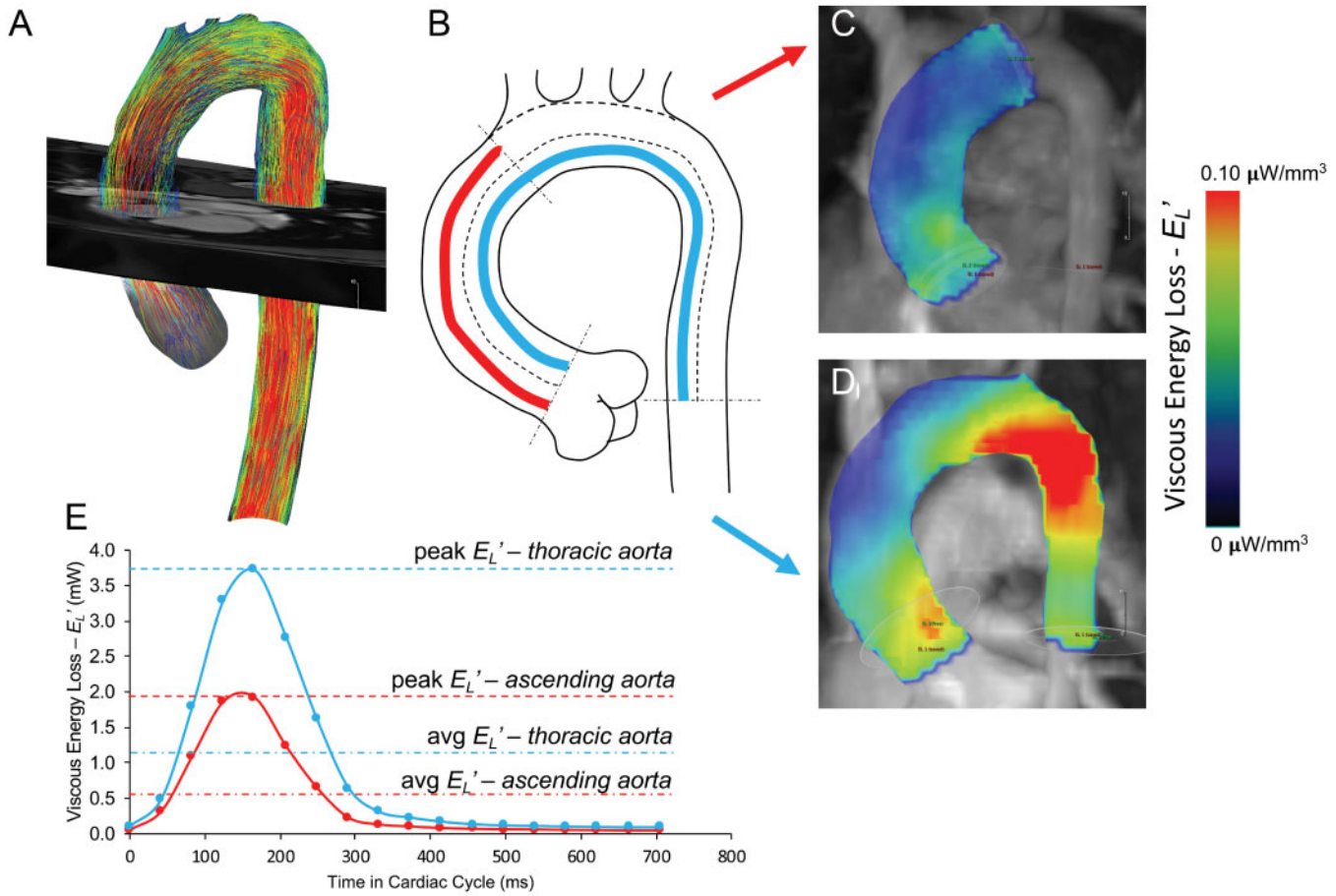

Figure 1: (**A**) Aortic contour was segmented from the initial 4-dimensional-flow dataset with separation of the head and neck vessels. (**B**) A luminal centreline was then created to delineate 2 anatomically standardized aortic regions: (1) ascending aorta (sinotubular junction to the first arch vessel origin) and (2) thoracic aorta (sinotubular junction to mid-descending aorta measured at the level of the aortic root). Viscous kinetic energy loss -E_L' represented by heat map visualization depicting the energy loss per voxel volume in the ascending aortic (**C**) and thoracic region (**D**).

resulting in temporal resolution between 38–48 ms and field of view (FOV): 250–320 × 200–250 mm^2 providing a voxel size = 2.0 × 2.0 × 2.0–2.8 mm^3 and velocity encoding 100–150 cm/s. Typical acquisition time was 8–15 min depending on heart rate and respiratory gating efficiency.

Viscous energy loss analysis

4D-flow datasets were imported into CVI42 platform (Version 5.9.1, Circle Cardiovascular Imaging, Calgary, AB, Canada) for viscous energy loss analysis. The entire dataset was corrected for background offset errors and velocity aliasing artefacts in each encoding direction per consensus recommendation [14]. Three-dimensional volume rendering of the phase-contrast MRI angiography derived from the 4D-flow dataset was created for detailed segmentation of the thoracic aorta. The head and neck vessels and LV outflow tract were excluded from the segmentation.

To calculate E_L', the centreline along the length of the thoracic aorta was used to identify the region of interest and delineate energy loss in a predefined volumetric region. The determination of instantaneous viscous energy loss due to frictional forces was previously described by Barker *et al.*, [12] where the rate of energy dissipation is calculated per individual voxel within a predefined region of interest by computation of the viscous component of the Navier–Stokes energy equation for incompressible fluid at any point in the cardiac cycle. This approach computes the viscous stress tensor per unit of volume (defined by voxel size) for an individual cardiac phase, under an assumption of uniform viscosity and boundary slip conditions. The instantaneous energy loss was quantified for: (i) the thoracic aorta extending from the level of the sinotubular junction to the mid-descending aorta (at the level of aortic root), (ii) the ascending aorta from the sinotubular junction to the origin of the brachiocephalic artery (or first arch vessel in the case of abnormal aortic arch arrangement) and (iii) the aortic arch and descending aorta (Fig. 1). Peak systolic and average energy losses per cardiac cycle were recorded yielding the instantaneous metric of power loss measured in milliWatts (mW).

Statistical analysis

Analyses were performed in Prism (version 7; GraphPad Software, La Jolla, CA, USA). Variables were checked for the distributional assumption of normality using normal plots, in addition to Kolmogorov–Smirnov and Shapiro–Wilks tests. Demographic and clinical characteristics between groups were compared using Student's *t*-test for normally distributed continuous variables. The Mann–Whitney *U*-test was used for non-normally distributed variables and the χ^2 test for categorical variables with no further

corrections for multiple testing. The relationship between the degree of energy loss and aortic stiffness and LV function was analysed by simple linear regression analysis using Pearson's correlation. Significance was based on *P*-value <0.05.

RESULTS

TOF and control demographics and LV haemodynamic characteristics are reported in Table 1. Thirty-six TOF subjects (88%) underwent primary complete repair (32 transannular patch, 3 valve sparing, 1 right ventricle to pulmonary artery conduit). Five patients (12%) had neonatal systemic-pulmonary shunts followed by shunt takedown and repair with right ventricle to pulmonary artery conduit. TOF arch sidedness was left in 27 patients (66%) and right in 14 (34%). The median age at repair was 8 months (range 0.8–60 months). All controls had normal left arch anatomy. No subjects took antihypertensive medications.

Table 1: Demographics and MRI haemodynamics

	TOF (*n* = 41)	Control (*n* = 15)	*P*-value
Age (years)	14 (10–21)	10 (10–18)	0.61
Female gender, *n* (%)	19 (46)	9 (60)	0.37
BSA (m^2)	1.28 ± 0.43	1.26 ± 0.32	0.66
LV-EDVi (ml/m^2)	84 (71–95)	76 (71–83)	0.34
LV-ESVi (ml/m^2)	38 (32–45)	32 (31– 5)	0.032
LV-SVi (ml)	46 (38–52)	43 (41–57)	0.08
LV-EF (%)	55 (52–57)	58 (55–62)	0.023
LV-CI (l/min/m^2)	3.3 (2.8–3.8)	3.7 (3.4–3.9)	0.123
RV-EDVi (m/s)	135 (113–154)	76 (73–96)	<0.001
RV-ESVi	67 (56–80)	34 (32–36)	<0.001
RV-EF	49 (45–55)	57 (56–62)	<0.001

Data are represented as median with corresponding interquartile range or mean ± standard deviation.

BSA: body surface area; CI: cardiac index; EDVi: end-diastolic volume index; EF: ejection fraction; ESVi: end-systolic volume index; LV: left ventricle; MRI: magnetic resonance imaging; RV: right ventricle; SV: stroke volume; TOF: tetralogy of Fallot.

With respect to LV volume and function, there were no differences in indexed end-diastolic volume and stroke volume (SV) between groups, but patients with TOF had increased indexed end-systolic volume (median 38 vs 32 ml/m^2, $P = 0.032$) and decreased LV ejection fraction (median 55% vs 58%, $P = 0.023$). There were no differences in cardiac index or LV mass index. As expected, patients with TOF had increased indexed right ventricular (RV) end-diastolic volume (median 135 vs 76 ml/m^2, $P < 0.001$), increased RV end-systolic volume (median: 67 vs 34 ml/m^2, $P < 0.001$) and decreased RV ejection fraction (median: 49% vs 57%, $P < 0.001$). Lastly, patients with TOF had increased ascending aortic size (mean ± standard deviation 2.5 ± 0.55 vs 2.0 ± 0.39 cm, $P = 0.002$).

Aortic viscous energy loss and flow analysis

The assessment of E_L' is summarized in Fig. 2 and Table 2. TOF subjects had increased peak systolic energy dissipation along the entire length of the thoracic aorta (median 3.8 vs 1.5 mW, $P = 0.004$). This finding persisted when adjusted for subject specific stroke volume (0.067 vs 0.029 mW/ml, $P = 0.012$). Similarly, average E_L' throughout the cardiac cycle was increased in TOF patients (1.2 vs 0.5 mW, $P = 0.003$). When analysis was confined to the ascending aorta, the results were similar with a 2-fold increase in systolic energy loss in the TOF group (2.0 vs 0.9 mW, $P = 0.007$). This finding persisted when adjusted to stroke volume (0.035 vs 0.019 mW/ml, $P = 0.020$). Average E_L' in the ascending aorta was also increased in the TOF group (0.7 vs 0.3 mW, $P = 0.003$). Lastly, E_L' in the aortic arch and descending aorta of the TOF group was greater (peak systolic E_L' 1.7 vs 0.7 mW,

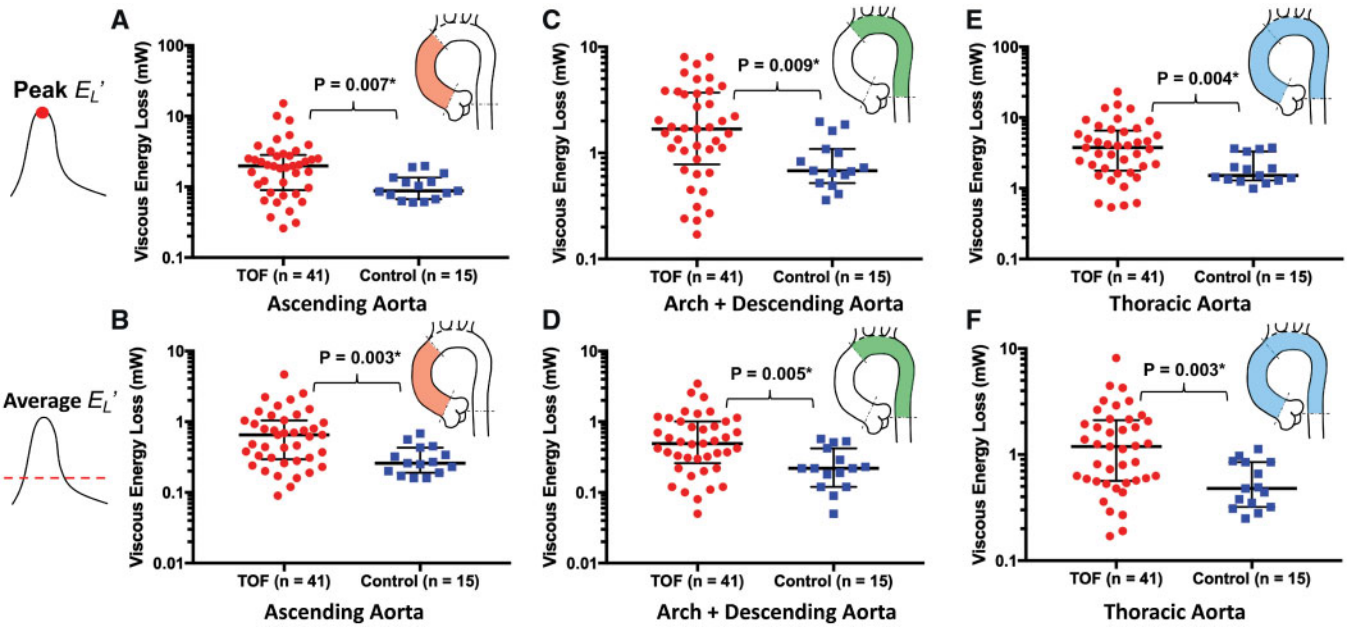

Figure 2: Peak systolic energy (**A**) and average E_L' (**B**) were significantly increased within the ascending aorta in subjects with TOF. Similarly, peak systolic E_L' was further elevated along the aortic arch–descending aortic tract (**C**) with no difference in the average E_L' in the same region (**D**). There was also increase in peak systolic and average E_L' along the entire thoracic aorta (**E**) and (**F**), respectively. TOF: tetralogy of Fallot.

CONGENITAL

Table 2: Aortic viscous energy (E'_L) loss

	TOF ($n = 41$)	Control ($n = 15$)	P-value
Thoracic aorta			
Peak systole (mW)	3.8 (1.8–6.6)	1.5 (1.3–3.3)	0.004
Peak systole/SV (mW/ml)	0.067 (0.042–0.097)	0.029 (0.025–0.059)	0.020
Average (mW)	1.2 (0.6–2.1)	0.5 (0.3–0.9)	0.003
Ascending aorta			
Peak systole (mW)	2.0 (0.9–2.8)	0.9 (0.7–1.4)	0.007
Peak systole/SV (mW/ml)	0.035 (0.022–0.054)	0.019 (0.014–0.034)	0.020
Average (mW)	0.7 (0.3–1.0)	0.3 (0.2–0.4)	0.003
Arch + descending aorta			
Peak systole (mW)	1.7 (0.8–3.7)	0.7 (0.5–1.1)	0.009
Peak systole/SV (mW/ml)	0.029 (0.017–0.053)	0.015 (0.009–0.024)	0.014
Average (mW)	0.5 (0.3–1.0)	0.2 (0.1–0.4)	0.005

Data are represented as median with interquartile ranges.
SV: stroke volume; TOF: tetralogy of Fallot.

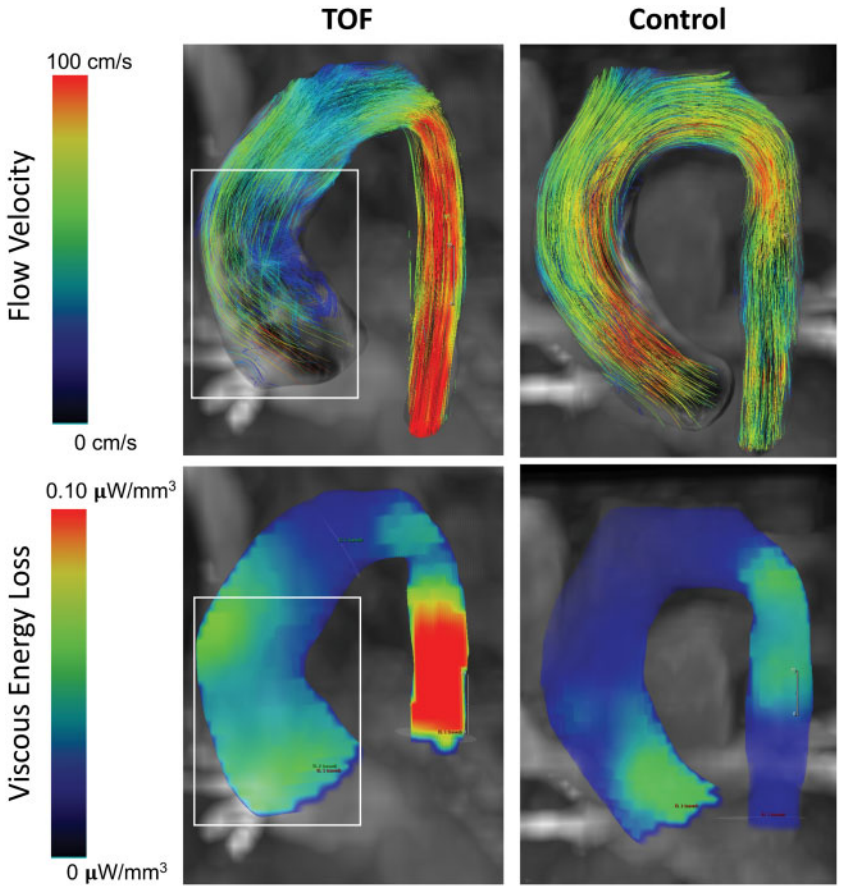

Figure 3: Comparative visualization of abnormal flow patterns and kinetic energy loss heat maps between a representative patient with TOF and a healthy control. Notice that regions with prominent secondary flow structures were associated with the elevated energy dissipation. One can further notice that viscous energy loss is associated with regions of flow acceleration typically present in the descending aorta. TOF: tetralogy of Fallot.

$P = 0.009$; SV adjusted peak systolic E'_L 0.029 vs 0.015 mW, $P = 0.014$).

Regions of prominent E'_L dissipation were associated with pathological aortic flow structures in TOF patients. These regions were characterized by prominent helical flow formations through systole along the inner curve of the ascending aorta (Fig. 3). Abnormal helical formations were present in 36 TOF patients (89%). Specifically, patients with TOF demonstrated a primary flow jet that exited the left ventricular outflow tract (LVOT) towards the outward anterior portion of the aortic wall. Simultaneously, secondary supraphysiological helices were formed along the inner curve of the ascending aorta typically at peak systole and enlarged towards the centre of the aortic lumen during the progression of systole (Fig. 4). Conversely, we observed that the single flow jet exiting the LVOT in control patients took a uniformly laminar pattern across the lumen of the

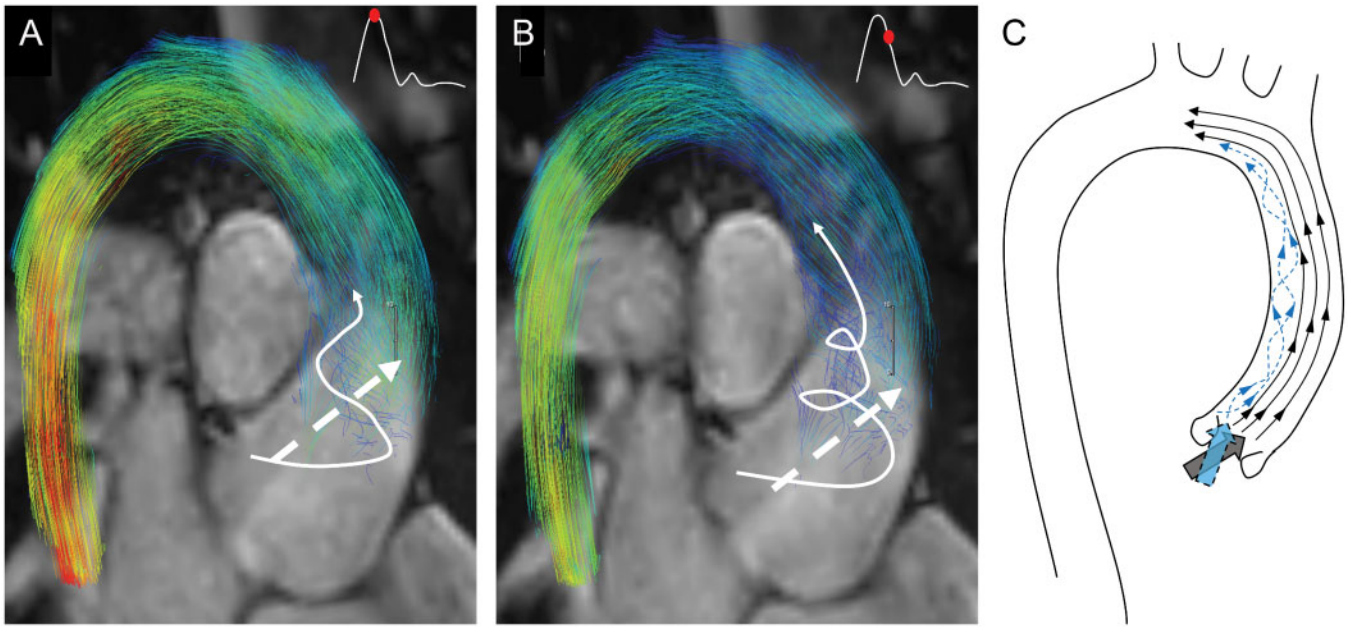

Figure 4: Abnormal flow formations in a child with repaired tetralogy of Fallot (TOF) superimposed to standard steady-state free precession magnetic resonance imaging images for better visualization of the aortic outflow tract–flow relationship at the peak systole (**A**) and late systole (**B**). Characteristic secondary supraphysiological helices formed along the inner curve of the aorta and enlarged through the aortic lumen during progression of systole (white arrow). Secondary helical flow formations then mix with the primary flow jet (dashed white arrow) at the proximal level of the aortic arch. (**C**) Artistic representation of streamlines present in the thoracic aorta of patient with TOF. Two prominent stream jets at the level of the left ventricular outflow tract result in laminar cohesive flow along the outer curvature of the aorta, and secondary helical flow along the inner curve.

Table 3: Correlation between E'_L with LV/RV haemodynamics and surgical repair

	Beta ± SE	*R*-value	*P*-value
LV-EF (%)	-2.78 ± 1.00	-0.45	0.009
LV-EDVi (ml/m^2)	2.81 ± 2.99	0.15	0.354
LV-ESVi (ml/m^2)	4.15 ± 1.54	0.40	0.010
LV-SV (ml)	-0.85 ± 1.89	-0.07	0.655
LV-CI (l/min/m^2)	-0.069 ± 0.152	-0.08	0.654
RV-EDVi (ml/m^2)	11.0 ± 6.14	0.28	0.080
RV-ESVi (ml/m^2)	9.67 ± 4.39	0.37	0.034
RV-EF (%)	-2.58 ± 1.50	-0.26	0.091
RF (%)	-0.88 ± 3.64	-0.04	0.809
Aortic size (cm)	-0.07 ± 0.11	-0.10	0.534
Age at repair (months)	-0.17 ± 0.23	-0.12	0.475

Data are reported as beta coefficients representing the best fit values from the linear regression ± standard error, Pearson *R*-value and respective *P*-value. E'_L values were natural log transformed for the correlation analyses.
CI: cardiac index; EDVi: indexed end-diastolic volume; EF: ejection fraction; ESVi: indexed end-systolic volume; LV: left ventricle; RF: pulmonary regurgitation fraction; RV: right ventricle; SV: stroke volume.

ascending aorta with no secondary flow patterns. All control patients had normal flow patterns with no secondary flow formations.

Aortic energy loss and flow haemodynamics

A summary of correlative analyses is depicted in Table 3 and significant correlations are portrayed in Fig. 5. Peak E'_L measured along the entire thoracic aortic length correlated with LV ejection fraction (R = -0.45, P = 0.009), indexed LV end-systolic volume (R = -0.40, P = 0.010), and right ventricular end-systolic volume (R = -0.37, P = 0.034). E'_L in the ascending aorta did not correlate with measures of aortic size. Finally, there was no association between E'_L and the time of surgical repair.

DISCUSSION

The long-term management of TOF is primarily concentrated on the status of the right heart [15], and left heart pathophysiology has largely been attributed to the concomitant impact of right heart dysfunction. Recent studies have demonstrated that TOF is associated with significant abnormalities of aortic wall physiology [5, 10, 16]. This study further demonstrates that in a relatively young cohort of patients with repaired TOF: (i) abnormal flow haemodynamic patterns are associated with elevated viscous energy loss $-E'_L$ through the thoracic aorta, and (ii) the magnitude of E'_L is associated with reduced LV function. The late impact of increased transaortic fluid mechanical energy loss on LV function in patients with repaired is unknown.

Altered flow haemodynamics in tetralogy of Fallot

Using 4D-flow MRI, unique aortic flow haemodynamic patterns have been described in paediatric and adult patients with aortic stenosis, dilation and in patients with aortic dissection [12, 17–20]. The common finding in these studies is that altered flow distribution correlates with abnormal aortic wall shear forces. In a prior study, we demonstrated that wall shear stress is elevated throughout the proximal aorta in preadolescent patients with repaired TOF even though aortic dimensions were normal [3]. Wall shear stress exerts major regulatory effects on arterial wall biology through endothelial mechano-transduction. These influences regulate intracellular signalling cascades responsible for

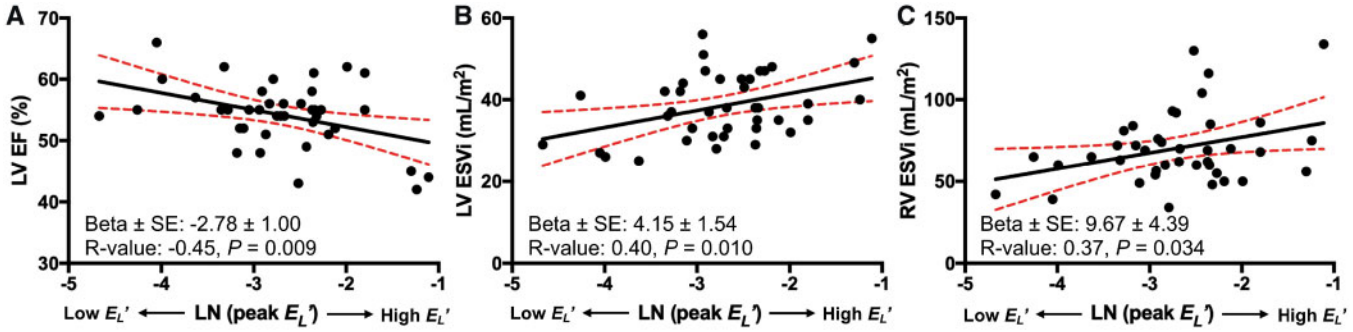

Figure 5: E_L' correlated in negative fashion with LVEF (**A**), and positively with left ventricular end-systolic volume index (**B**), and right ventricular end-systolic volume index (**C**). ESVi: end-systolic volume index; LN: natural logarithm; LV: left ventricle; LVEF: left ventricular ejection fraction; RV: right ventricle; SE: standard error.

endothelial arrangement, proliferation and even paracrine signalling associated with smooth muscle cell proliferation and extracellular matrix alterations [21].

Abnormal aortic valve anatomy such as bicuspid valve or any form of aortic valve stenosis impacts flow haemodynamic characteristics in the proximal aorta. In prior work, Barker *et al.* [11] demonstrated unique flow jet patterns in bicuspid aortic valve patients and directly linked unique flow patterns to the pattern of cusp fusion. Barker *et al.* [12] subsequently associated abnormal aortic flow with increased E_L' in patients with aortic stenosis. Our findings indicate that most TOF patients (89%) have a primary systolic flow jet that exits the LVOT towards the outward anterior portion of the aortic wall. These patients also form secondary supraphysiological helices along the inner curve of the ascending aorta that enlarges towards the centre of the aortic lumen during the progression of systole (Fig. 4). In the proximal aortic arch, the secondary helical flow formation mixes with the primary flow jet. In our experience with 4D-flow MRI assessments in numerous forms of congenital heart disease, this flow haemodynamic abnormality is unique to patients with repaired TOF.

Causal factor(s) of the perturbed flow pattern and associated elevated E_L' prevalent in the TOF group are not known. In other studied lesions, causes of secondary flow structures (helices and vortices) and energy loss include: (i) altered LVOT anatomy (e.g. aortic stenosis), and (ii) aortic dilation [11, 12, 19]. All patients in our TOF cohort had non-stenotic tri-leaflet aortic valves. In prior studies increased E_L' was present in patients with ascending aortic aneurysms and aortic valve stenosis [12]. Additional studies have associated abnormal aortic geometry post extensive surgical reconstruction in Norwood procedure with increased E_L' and abnormal flow haemodynamic patterns [22]. The lack of association between E_L' and ascending aortic size in our TOF cohort is likely due our exclusion of patients with sizes above the normal range ($z < 2$). Therefore, abnormal aortic leaflet anatomy and aortic dilation do not explain our findings. Furthermore, we did not observe any association between E_L' and the time of surgical repair.

TOF is characterized by the presence of a large subaortic ventricular septal defect, and the aortic valve is dextroposed resulting in anterior malalignment of the aortic root above the ventricular septum. Surgical closure of the ventricular septal defect directs LV output to the aorta along a pathline that differs significantly from normal anatomy. We speculate that this abnormality of the left ventricular outflow tract in TOF is the primary factor that explains our findings. The anatomic features of TOF occur in a spectrum. Consequently, patients with more mild features of TOF (i.e. less aortic override and less subpulmonary right ventricular outflow tract obstruction) would have more normal LVOT anatomy following repair, which could explain the absence of abnormal flow haemodynamic patterns in the minority of TOF patients we studied. However, the effect of specific TOF pathologies and surgical strategy on the late outcome of aortic flow haemodynamics require further investigations.

Energy loss and left ventricular function

LV function is an important prognostic marker of late mortality and morbidity in TOF [23]. The difference in aortic E_L' loss at rest in TOF patients compared with normal controls constitutes irreversibly wasted LV mechanical energy that is converted to heat. All studies were performed in the resting state, and the magnitude of wasted energy would likely be significantly increased during physiological conditions requiring greater metabolic demand (e.g. exercise). As a result, inefficient LV energy expenditure may adversely impact late survival. Typical resting LV power output can be derived as a product of cardiac index and mean arterial blood pressure and varies between 0.5 and 1.0 W. Using this estimate, the flow related energy loss observed in our TOF cohort ranged between 0.1% and 5.4% of power provided by cardiac energetic output at peak systole [12]. However, this metric does not consider the energetic expenditure throughout the entire cardiac cycle and does not account for the energy loss associated with turbulent structures. Lastly, the effect of E_L' on exercise and age progression is unknown.

Based on left ventricular ejection fraction (LVEF), the observed relationship between calculated energy loss and LV function was very modest, and the majority of TOF patients had clinically normal LVEF. However, LVEF is not a sensitive measure, and compromised myocardial deformation can occur without a parallel reduction in LVEF [24]. Theoretical work by Stokke *et al.* [24] demonstrated that geometric effects represented by myocardial thickening can compensate for decreased longitudinal and circumferential strain early in the disease process indicating that early systolic dysfunction can be present without a major change in ejection fraction. Sjöbert *et al.* [25] analysed LV systolic performance in patients with repaired TOF using 4D-flow MRI and found significantly reduced kinetic energy production in an assessment confined to the LV cavity. The interplay between kinetic energy concentrated in the flow domain inside the LV during systole and E_L' the ascending aorta remains unexplored. It is likely that compromised LV contractile function associated with mechanical and electrical dyssynchrony combined with abnormal LVOT morphology generates a suboptimally ejected stroke volume bolus resulting in wasted flow-mediated kinetic energy.

Limitations

This study has several limitations. First, we did not consider turbulent kinetic energy which involves voxel by voxel analyses of temporal flow fluctuations and is often a significant contributor of flow turbulence. This method requires a separate reference velocity encoding step in order to detect velocity fluctuation signalling [13]. In addition, turbulent kinetic energy calculations tend to omit large scale secondary flow formations which are typically present in aortopathies such as those observed in this study. Consequently, our energy loss calculations most likely underestimate the true energy loss to the system. Second, all patients with TOF underwent at least 1 cardiac operation and many experienced cyanotic states from birth until complete repair was undertaken. These factors could potentially contribute to the observed minor decrease in LV function in the TOF group, and the impact of these differences compared with controls is impossible to determine. Third, we were not well equipped to perform the flow haemodynamic comparison between different TOF lesions and initial surgical approach. Our future studies will focus on investigating the aortic flow haemodynamic outcomes with regard to the surgical strategy, aortic root geometry and late clinical outcomes.

CONCLUSION

In conclusion, patients with repaired TOF have abnormal flow conduction through the proximal thoracic aorta that is associated with significantly increased E'_L loss compared with normal age-matched controls. These findings are marked, but the long-term ramifications on LV function and clinical outcome are unknown because no cohort of patients undergoing early complete repair of TOF has reached more advanced age. The potential negative impact of wasted LV energy expenditure during the propagation of aortic blood flow in patients with TOF repaired early in life warrants further investigation.

ACKNOWLEDGEMENTS

This study was supported by a generous gift from the Rady Family Foundation and Jayden DeLuca Foundation. A.J.B. is supported in part by NIH K25HL119608 and R01HL133504.

Conflict of interest: none declared.

REFERENCES

[1] Cheung YF, Ou X, Wong SJ. Central and peripheral arterial stiffness in patients after surgical repair of tetralogy of Fallot: implications for aortic root dilatation. Heart 2006;92:1827–30.
[2] Tan JL, Davlouros PA, Mccarthy KP, Gatzoulis MA, Ho SY. Intrinsic histological abnormalities of aortic root and ascending aorta in tetralogy of Fallot evidence of causative mechanism for aortic dilatation and aortopathy. Circulation 2005;112:961–9.
[3] Schäfer M, Browne LP, Morgan GJ, Barker AJ, Fonseca B, Ivy DD *et al.* Reduced proximal aortic compliance and elevated wall shear stress after early repair of tetralogy of Fallot. J Thorac Cardiovasc Surg 2018;156:2239–49.
[4] Chowdhury UK, Mishra AK, Ray R, Kalaivani M, Reddy SM, Venugopal P. Histopathologic changes in ascending aorta and risk factors related to histopathologic conditions and aortic dilatation in patients with tetralogy of Fallot. J Thorac Cardiovasc Surg 2008;135:69–77.
[5] Senzaki H, Iwamoto Y, Ishido H, Matsunaga T, Taketazu M, Kobayashi T *et al.* Arterial haemodynamics in patients after repair of tetralogy of Fallot: influence on left ventricular after load and aortic dilatation. Heart 2008;94:70–4.
[6] François K, Creytens D, De Groote K, Panzer J, Vandekerckhove K, De Wolf D *et al.* Analysis of the aortic root in patients with tetralogy of Fallot undergoing early repair: form follows function. J Thorac Cardiovasc Surg 2014;148:1555–9.
[7] Niwa K, Siu SC, Webb GD, Gatzoulis MA. Progressive aortic root dilatation in adults late after repair of tetralogy of Fallot. Circulation 2002;106:1374–8.
[8] Tan JL, Davlouros PA, McCarthy KP, Gatzoulis MA, Ho SY. Intrinsic histological abnormalities of aortic root and ascending aorta in tetralogy of Fallot: evidence of causative mechanism for aortic dilatation and aortopathy. Circulation 2005;112:961–8.
[9] François K, Zaqout M, Bové T, Vandekerckhove K, De Groote K, Panzer J *et al.* The fate of the aortic root after early repair of tetralogy of Fallot. Eur J Cardiothorac Surg 2010;37:1254–8.
[10] Shiina Y, Murakami T, Kawamatsu N, Niwa K. Aortopathy in adults with tetralogy of Fallot has a negative impact on the left ventricle. Int J Cardiol 2017;228:380–4.
[11] Barker AJ, Markl M, Bürk J, Lorenz R, Bock J, Bauer S *et al.* Bicuspid aortic valve is associated with altered wall shear stress in the ascending aorta. Circ Cardiovasc Imaging 2012;5:457–66.
[12] Barker AJ, van Ooij P, Bandi K, Garcia J, Albaghdadi M, Mccarthy P *et al.* Viscous energy loss in the presence of abnormal aortic flow. Magn Reson Med 2013;628:620–8.
[13] Dyverfeldt P, Hope MD, Tseng EE, Saloner D. Magnetic resonance measurement of turbulent kinetic energy for the estimation of irreversible pressure loss in aortic stenosis. JACC Cardiovasc Imaging 2013;6:64–71.
[14] Dyverfeldt P, Bissell M, Barker AJ, Bolger AF, Carlhäll C-J, Ebbers T *et al.* 4D flow cardiovascular magnetic resonance consensus statement. J Cardiovasc Magn Reson 2015;17:72.
[15] Stout KK, Daniels CJ, Aboulhosn JA, Bozkurt B, Broberg CS, Colman JM *et al.* 2018 AHA/ACC guideline for the management of adults with congenital heart disease. J Am Coll Cardiol 2018;18:S0735–1097.
[16] Chong WY, Wong WHS, Chiu CSW, Cheung YF. Aortic root dilation and aortic elastic properties in children after repair of tetralogy of Fallot. Am J Cardiol 2006;97:905–9.
[17] Allen BD, Van Ooij P, Barker AJ, Carr M, Gabbour M, Schnell S *et al.* Thoracic aorta 3D hemodynamics in pediatric and young adult patients with bicuspid aortic valve. J Magn Reson Imaging 2015;42:954–63.
[18] Binter C, Gotschy A, Sündermann SH, Frank M, Tanner FC, Lüscher TF *et al.* Turbulent kinetic energy assessed by multipoint 4-dimensional flow magnetic resonance imaging provides additional information relative to echocardiography for the determination of aortic stenosis severity. Circ Cardiovasc Imaging 2017;10:e005486.
[19] Bürk J, Blanke P, Stankovic Z, Barker A, Russe M, Geiger J *et al.* Evaluation of 3D blood flow patterns and wall shear stress in the normal and dilated thoracic aorta using flow-sensitive 4D CMR. J Cardiovasc Magn Reson 2012;14:84.
[20] Hope TA, Kvitting JPE, Hope MD, Miller DC, Markl M, Herfkens RJ. Evaluation of Marfan patients status post valve-sparing aortic root replacement with 4D flow. Magn Reson Imaging 2013;31:1479–84.
[21] Davies PF. Hemodynamic shear stress and the endothelium in cardiovascular pathophysiology. Nat Rev Cardiol 2009;6:16–26.
[22] Schäfer M, DiMaria MV, Jaggers J, Mitchell MB. Suboptimal neoaortic arch geometry correlates with inefficient flow patterns in hypoplastic left heart syndrome. J Thorac Cardiovasc Surg 2019;158:e113.
[23] Diller GP, Kempny A, Liodakis E, Alonso-Gonzalez R, Inuzuka R, Uebing A *et al.* Left ventricular longitudinal function predicts life-threatening ventricular arrhythmia and death in adults with repaired tetralogy of Fallot. Circulation 2012;125:2440–6.
[24] Stokke TM, Hasselberg NE, Smedsrud MK, Sarvari SI, Haugaa KH, Smiseth OA *et al.* Geometry as a confounder when assessing ventricular systolic function: comparison between ejection fraction and strain. J Am Coll Cardiol 2017;70:942–54.
[25] Sjöberg P, Bidhult S, Bock J, Heiberg E, Arheden H, Gustafsson R *et al.* Disturbed left and right ventricular kinetic energy in patients with repaired tetralogy of Fallot: pathophysiological insights using 4D-flow MRI. Eur Radiol 2018;28:4066.